

TRD PROJECT 5

ENGINEERING DEVELOPMENTS FOR HIGH AND ULTRAHIGH FIELD MRI AND MRS

THOMAS VAUGHAN (TRD PI)

GREGOR ADRIANY

LANCE DELABARRE

DEVASHISH SHRIVASTAVA

CARL SNYDER

JOHN STRUPP

JINFENG TIAN

KAMIL UGURBIL

SPECIFIC AIMS AND THE RESEARCH STRATEGY

A. SPECIFIC AIMS

The objective of TRD 5 is to provide engineering solutions and support to all TRDs and to various collaborative and service projects in this BTRC. To fulfill its objective, the engineering group of TRD 5 must invent, develop, implement and improve entirely new technologies required to make MR signal acquisition possible, safe and successful for a wide variety of new biomedical applications employing high and ultrahigh magnetic field strengths. This TRD will also provide service by supplying necessary hardware, such as RF coils, using already established technologies. Service also includes dissemination of technology and knowhow through publication, technology transfer, workshops and training.¹⁻³⁹ More specifically, innovative new multi-channel head coils combining large numbers of transmit, receive, and transceive elements distributed over three dimensions including in the “z” axis will be developed for highly sensitive, ultrahigh field neuroimaging of brain function, anatomy and connectivity for TRD 1 and for their collaborations such as the Human Connectome Project. TRD Project 2 will require additional innovation in coil design to exclude or shield the proton signal excited in traditional coil building and packaging materials in order to support the development of novel MRI sequences with frequency-swept pulses. B₁ field management through parallel transmission in TRD 3, a spin-off technology of TRD 5 R&D in previous years, requires RF transmitters and coils of numerous, independently driven and controlled transmit elements distributed in x, y, and z dimensions to give full control over the phase, magnitude, space, time, and frequency of the field within the sample space of the coil. Ultrahigh field body MRI was not considered possible until first demonstrated by our center and the engineers of TRD 5. Being still very new, significant new technology development is proposed to meet the challenges and reap the benefits of whole body imaging at 3T and 7T for TRD 4. To facilitate these new imaging technologies and methods for the TRDs and their collaborations, intelligent interfaces must be designed to control, power, excite and receive from the new coil designs proposed. Additional new concepts in RF coil design, application, and integration with B₀ shim and gradient systems will continue to expand MR system capabilities. Adding to the challenge, the efforts above will be multiplied with the addition of a 10.5T whole body system expected to be operational in early 2013. A “Safety” Aim will meet the IRB, IDE and general safety requirements for the new technologies and applications proposed. These TRD 5 objectives will be achieved by the following Aims.

Aim 1. Technology for High Field Head, Limb and Animal Imaging

- 1.1 Multichannel Receive Arrays for
 - a. 3T & 7T human applications
 - b. 9.4T, 16.4T animal applications
- 1.2 Multichannel Transceive Arrays
 - a. 3T, 7T, 10.5T human applications
 - b. 9.4T, 16.4T animal applications

Aim 2. Technology for Body Imaging

- 2.1 Body Surface Coil for 3T & 7T human applications
- 2.2 Body Volume Coil for 3T & 7T human applications

Aim 3. RF Coil Interface and Control Circuits

- 3.1 Auto-tune and match
- 3.2 On-coil power amps
- 3.3 On-coil power monitoring

Aim 4. New RF Concepts

- 4.1 Dynamic, feedback driven isolation for continuous SWIFT
- 4.2 Dielectrics for RF lensing and impedance matching
- 4.3 Locally integrated shims, gradients, and RF coils

Aim 5. RF Safety

- 5.1 Modeling SAR and Temperature
- 5.2 RF safety protocol implementation
- 5.3 Development of new RF safety protocol
- 5.4 Development of NMR thermometry methods

B. SIGNIFICANCE

The rationale for the TRD 5 objective to advance ultrahigh field technology in support of the TRD Projects and Collaborators is based on the demonstration, largely coming from our Center, that (i) ultrahigh fields provide unique information that is not available at lower magnetic fields, (ii) such information can be obtained not only in the human brain but, with appropriate technological developments, in the human torso and extremities as well, and (iii) such information is useful both for basic biomedical and translational research as well as for clinical medicine. Specific demonstrations at 7T and 9.4T include:

- SNR gains in the human brain at such high magnetic fields (a concept that was previously questioned)^{40,41},
- the feasibility of improved morphological imaging^{40,42},
- significantly improved fMRI contrast and accuracy⁴³⁻⁵⁵,
- higher resolution neurochemical spectroscopy⁵⁶⁻⁵⁹,
- improved parallel imaging⁶⁰⁻⁶²,
- feasibility of imaging in the human torso^{63,64}.

The crux of the problem toward which much of TRD 5 efforts are focused is related to the short Larmor wavelengths of the proton Larmor frequencies employed for ultra high field imaging. At frequencies of 128 MHz (3T) to 450 MHz (10.5T) coil circuits and human anatomy become multiple wavelengths in dimension. At these wavelengths, fields are significantly refracted, reflected, and attenuated in the coil circuit and tissue loads. Heat, noise, field non uniformity and loss result. These short waves also interfere in tissue, both constructively and destructively. These interference patterns further significantly degrade the spatial uniformity and signal for both transmit and receive fields in a physiological sample within the coil. Acquiring a head and especially a body image by conventional circularly polarized volume coils with or without local received arrays, and by conventional imaging methods will not give optimal results. To solve these problems a new method of imaging that could correct or mitigate field non uniformities and losses had to be invented. B_1 shimming, originally described as a method to modulate a field in not only phase and magnitude, but also in time, space and frequency in order to optimize a field over an ROI for any B_1 dependent parameter including SNR, SAR, uniformity/localization, speed and contrast, was developed and demonstrated by the TRD 5 group at 4T, 7T, and 9.4T in head and body applications. An additional “benefit” of the short wavelengths at higher fields is parallel imaging performance which reaches optimum conditions for head and body imaging at 7T and above. Through the new technology achieved, pursued and proposed by TRD 5, the problems of B_1 field losses and nonuniformities can be “managed” and the benefits can be realized to render more powerful MRI systems for this Center, for collaborators, and for the community.

The work of TRD Project 5 has already made significant impact toward realizing the inherent potential of ultrahigh field MRI and NMR. Historically the engineering team, comprised of TRD 5 and its collaborators, has achieved a number of important firsts in the field. The first 7T head imaging, the first 4T body imaging, the first 7T body imaging, and the first 9.4T human imaging are a few of the more notable. To make these landmarks in ultrahigh field human imaging possible, new methods and technologies had to be discovered, invented, developed and successfully applied. B_1 shimming was first applied in the human body to correct for B_1 artifacts in the heart at 4T, and then at 7T. Modern, console controlled B_1 shimming with programmable phase and gain control and multiple channel dedicated transmitters was first implemented to achieve the first 9.4T human head images. Of course entirely new coil designs had to be conceived and developed to accommodate these new approaches to ultrahigh field imaging. Some of the earliest examples of multi-channel, parallel transmit coils were developed for head and body imaging at 7T, and 9.4T, by this group. To assure that human imaging by these new technologies and techniques at unprecedented field strengths is safe, the TRD Project 5 has developed a new bioheat model, numerical methods, and an in vivo animal model to better understand, predict, monitor RF heating.^{1,17,65,66} TRD 5 continues with its highly productive track record.

While immediate clinical utility is not the focus of this grant application, it is the ultimate beneficiary. For example, multi-channel and B_1 shimming technologies are now being incorporated into the newest generations of clinical imagers. The scientific and engineering knowledge gain resulting from TRD 5 and the BTRC it supports will be directly applied to diagnostics and therapy protocols for mental health, neurological diseases, cardiovascular diseases, and cancer. The methodological and technological innovations developed will be

incorporated into clinical protocols and systems. Additional and more specific examples of scientific and clinical impact, immediate and eventual follow in the next sections.

C. Innovation

3T is the highest field strength used for clinical MRI. According to Frost and Sullivan, May 2010, sales of 3T units make up the fastest growing MRI systems market with approximately 2000 installed worldwide. 7T is the highest field for "standard" factory supported systems with approximately 40 of these systems installed. Four 9.4T systems exist, and one 11.7T, 68 cm bore (head only) system installed at the NIH. Due primarily to technological and methodological shortcomings, most of the human 7T and 9.4T systems are used only for heads. In particular, commercial RF head coils are not available for fields of 9.4T and higher, and commercial body coils are not available for 7T or above. A whole body 10.5T system is being delivered to the CMRR (Figure 10) which will need new coils as well as supporting RF front end technology. There are many additional technological and physical challenges to human imaging at these highest field strengths and Larmor frequencies that will be addressed by TRD 5. The Larmor wavelengths in the human tissue dielectrics at 300 MHz (7T) and 450 MHz (10.5T) are on the order of 12 cm and 8 cm respectively in high water content tissues such as muscle and brain. By conventional methods and thinking, these wavelengths would preclude any possibility of achieving safe and successful human-scale imaging. RF interference patterns from conventional, uniform field volume coils create severe RF field inhomogeneity in the anatomy. RF losses to the tissue result in severe heating for conventional pulse protocols. Conventional RF coil and frontend circuits are highly radiative (inefficient) with poor current and field control. New methods and technology being developed at Minnesota may not only solve some of these problems, but actually use the short wavelengths to new advantage. Examples of some of the new innovations proposed and being developed for solving high field problems follow.

1.) New head coil systems: Existing approaches can't accomplish successful inversion-recovery imaging of the whole head at these fields. Significant innovation will be required for a successful design. The coil systems proposed will include short, efficient, "3D", shielded coil element arrays, using linear elements for transmit and orthogonally decoupled loop element receivers. The elements will be electronically tuned and matched (Figure 5). On-coil decoupling preamps, power amplifiers, and transmit/receive (TR) switches are design goals. As many as 32 transmit channels and 64 receive channels will be distributed in x, y, and z for "3D" B_1 shimming.^{67,68} The coil includes practical features such as a front to back view port, and a compact diameter (32 cm) that fits into a head gradient coil set, such as a prototype shown in Figure 1.

2.) New body coil systems: Other than at the CMRR, a whole body volume coil does not exist for 7T. Figure 2 shows a 16 channel, 7T body coil, half of a 32 channel receiver, and a single frame of a B_1 and B_0 shimmed, cardiac cine acquired with the 16 channel transceive, 32 channel receive system.

Proposed here is a 7T, 48 channel body coil together with a 48 channel receive array set. Similar to the head coil above, the proposed body coil will incorporate on-coil power amps, preamps, TR switches, feedback driven auto-tuning circuitry, and elements distributed in x,y,z "3D" for improved B_1 uniformity control and SAR minimization (Figures 3,4,5,6).

3.) Novel coil element decoupling: The 48 channel TEM elements must be decoupled to 20 dB or better for parallel imaging and B_1 shimming performance. A new method for cancelling mutual inductance \mathbf{M} between elements with shield capacitance, \mathbf{C} , is proposed in Figure 3 (right) and will limit losses and field perturbations associated with conventional capacitive bridging as shown (left).^{67,68}

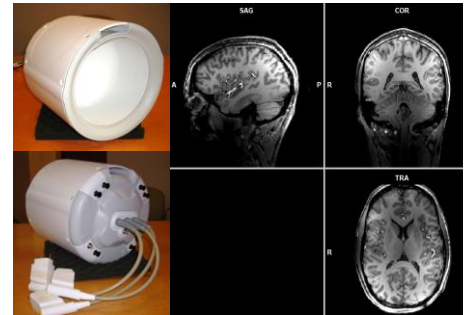


Figure 1. 7T head coil with 8 transmit and receive channels and 24 receive channels, totaling 32 receivers.

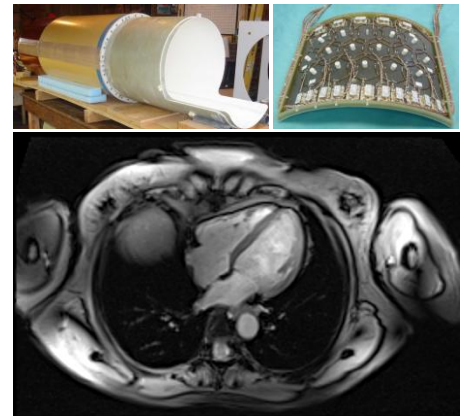
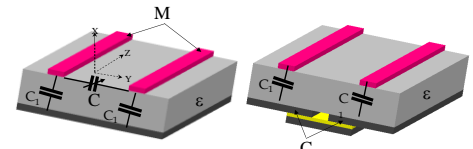


Figure 2. 16 channel, 7T body coil with 1/2 of a 32 channel receiver.

4.) On-coil power amplifiers are a new innovation: Due to cabling issues, power loss, and prohibitive expense of high-power amplifiers, it's difficult to imagine a 48 element 3D coil without local, on-coil power amplifiers. To test feasibility of this concept, class AB linear power amplifiers were tested in the magnet with a single amplifier driving a single TEM element to image a phantom. See Figure 4. Proposed is a more compact, significantly more efficient class E nonlinear power amplifier that can be pre-compensated for linear output and mounted right on a coil element. This innovation alone has the potential to revolutionize coil and MR system design.

5.) Auto tuning and matching: Automatic tuning and matching are also highly innovative and needed. An ultra-high frequency, multichannel transmit coil ideally must be tuned and matched per subject. Currently in the lab this is done manually, one element at a time. Note in Figure 4 the 16 tuning and 16 matching stems that must each be adjusted for each scan. This is difficult and time consuming. The coils proposed with twice the element count and inaccessible elements would make such manual adjustments impossible. The RF signal feedback driven, PIN diode switched, capacitance matrices for tuning and matching each coil element electronically, automatically with algorithm control, Figure 5, is therefore an innovation needed for the coils proposed, and for all practical multi-channel, transmit coils. This innovation also has immediate clinical relevance. Coil transmit efficiency and receive sensitivity on all systems would benefit by this technology.



$$M = \frac{\phi_{21}}{I_1} = \frac{\mu_0}{4\pi} \iiint_{\text{vol}} \left[\iint_{\text{vol}'} J \left[\frac{j\beta}{r'} + \frac{1}{r'^2} \right] e^{-j\beta r'} \frac{x-x_0}{r'} dy_0 dz_0 \right] dx dz$$

Figure 3. Decoupling coil elements, **M** with **C** by the usual practice (left) compared to the proposed method using shield capacitance **C** (right).

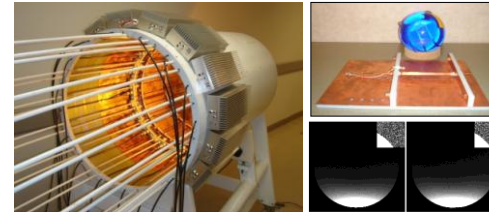


Figure 4. Local power amps mounted on multi-channel, 7T body coil (left). Single TEM element (top right) used to acquire phantom image with local amplifier (a) and with remote amplifier (b). Identical image (a) was acquired with 1/2 power of image (b).

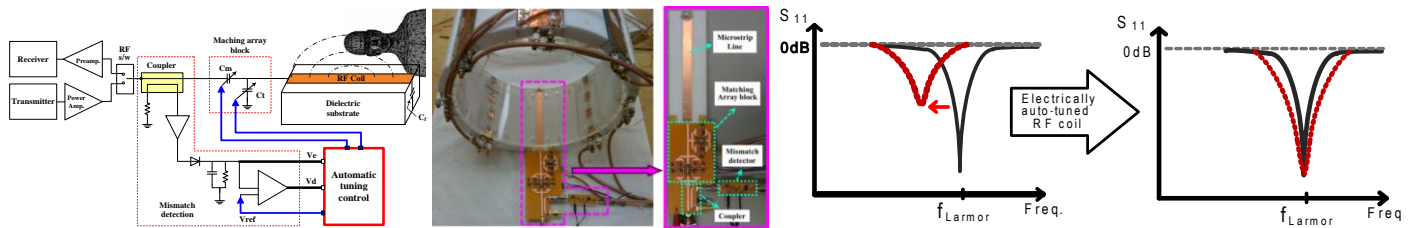


Figure 5. Electronic auto-tuning. Every channel in a multi-channel coil must be electronically tuned and matched per subject for best results. A feedback algorithm driven, PIN switched capacitance matrix adjusts frequency tune and impedance match per element, in situ. The diagram (left) details the circuit, the photo shows a prototypical implementation of the circuit on a single coil element. Model tune and match results are presented (right).

6.) On-coil transceiver: Extending from Figure 4 technology above, a high performance, low cost solution, integrated power modulator units, will be designed, built and implemented in the new head and body coils of this proposal. Combined with the preamplifiers in the coil, a high speed parallel transceiver will be developed and implemented. The new system proposed will reduce current command cycle delays to a sub-microsecond control cycle to facilitate SWIFT, Transmit SENSE, automated shimming and other high speed applications requiring high-speed switching and on-the-fly waveform modulation and feedback control. The broadband power amplifiers and other system components also allow for simultaneous or interleaved multi-nuclear applications, swept frequency methods, and other frequency dependent protocols. At the heart of this second generation parallel transceiver proposed is a transmitter module consisting of a single chip modulator, and a single Field Effect Transistor (FET) power amp, Figure 6. The compactness of this unit (~ 1 x 2 x 3 cm) will make it possible to integrate this unit with its dedicated coil element. Together with a similarly compact PIN diode protected preamp, this second generation parallel transceiver will be integrated at the probe head (coil) for maximum RF speed, performance and flexibility. A coil with

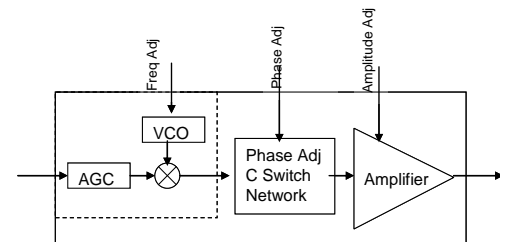


Figure 6. RF Analog IC, integrating power FET with phase and gain control, together with TR switch and preamp.

local phase, gain, frequency, temporal, and spatial (per element) control will bring a true paradigm shift to the concept of an RF coil and equally to a new family of RF sequences to take advantage of this new technology.

7.) **3D Coils:** Multi-channel transmit coil elements can be arrayed over three dimensions on the surface of a cylinder or other form to facilitate better control over the B_1 excitation field in x, y, and z. This gives yet another alternative approach that can be used alone or in combination with other approaches to maximize B_1 excitation uniformity and to minimize SAR peaks. In Figure 7, B_1 and SAR were calculated in a 72 kg male loading two, same dimension variations of a 16 channel TEM body coil, a “2D” coil with single ring of sixteen, 35 cm long TEM elements and a “3D” coil with two rings of eight, 17 cm elements with 1 cm spacing between the rings. All results are normalized to global SAR. The models clearly predict significant B_1 uniformity and dampened SAR peaks achieved with B_1 shimmed, 3D coils over non B_1 shimmed 2D coils.

8.) **New methods of modeling the human body** at unprecedented frequencies. See Figure 8. The success of coil systems’ design and operation will depend heavily on new approaches to modeling. Modeling RF field propagation and losses of multiple wavelengths in human anatomy is required for safe and successful imaging. Safety can no longer rely on coarse calculations of E-fields and SAR alone as is the current practice. Numerical predictions of heating (ΔT) and temperature contours (T) must be included. These thermal models must be accurate and precise to 0.2°C. The accuracy and precision of SEMCAD X, an FDTD solver, (Zurich, CH)⁶⁹ will be corrected by our bioheat equation¹, and validated in Collaboration 10 supporting whole body experiments with porcine models.⁷⁰ Even new body coils and methods recently developed for 7T (Figures 4, 13) must be redesigned to correct for increasingly nonuniform B_1^+ excitation fields and excessive heating in the arms, shoulders and neck predicted at 10.5T. See Figure 8.

9.) **Porcine Anatomy Atlas:** In order to validate thermal models with direct measurements, a porcine anatomy atlas will be created. Examples of segmented anatomy derived from MRI of a pig are shown in Figure 9. The World Health Organization recommends porcine models for investigations of RF dosimetry, heating, and heat stress.⁷¹

10.) **Highest field, whole-body magnet:** These magnets are uniquely innovative, Figure 10. While this proposal does not include magnet design, the fields generated by these magnets necessitate the many new innovations in the hardware and in the experiment protocols herein.

D. APPROACH

TRD Project 5 Progress 2008-2012

The Aims set forth for TRD Project 5 in the previous funding cycle were largely accomplished and reported.¹⁻
12,14-39,72

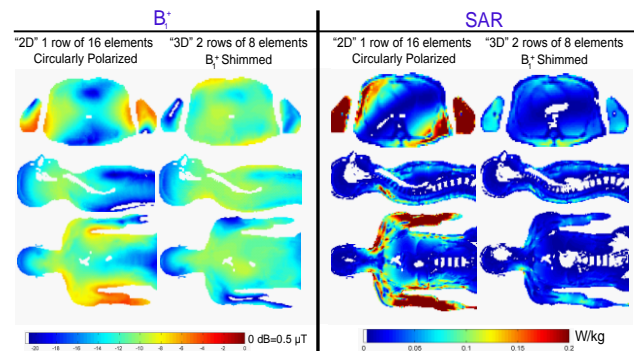


Figure 7. Optimization B_1^+ uniformity and minimization of SAR at 3T by multi-channel 3D element distribution on a whole body volume coil.

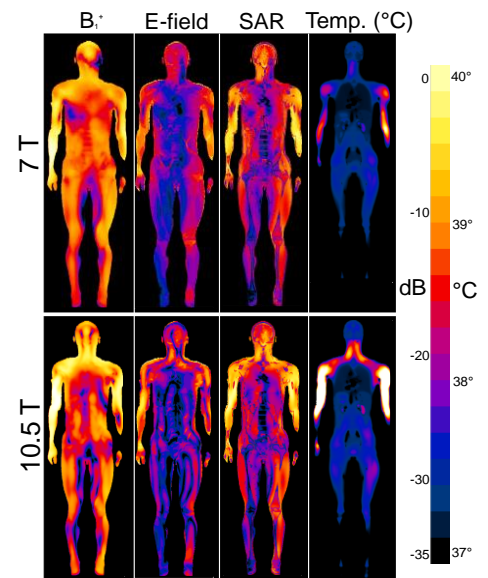


Figure 8. Human atlas showing B_1 , E, SAR, Temperature at 7T, 10.5T.

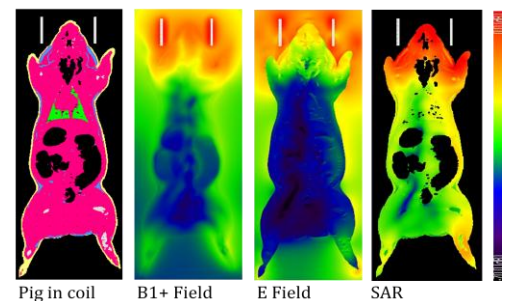


Figure 9 shows the center slice pig anatomy, B_1 fields, E fields, and SAR in 3D.

Aim 1, to develop new technology for head and animal imaging and spectroscopy from 3T to 9.4T was achieved through the design, modeling, and construction of new coils and B_1 field control systems, followed by their successful testing, evaluation, and implementation for applications of the other TRD projects and collaborations.^{2-7,10,11,28,31,32,34-39}

One such example of a successful multichannel head coil is the 8 channel transceiver by 24 channel receive coil system shown in Figure 1 above. Figures 11, 12 also show examples of design, test and evaluation approaches developed in Aim 1. Other head coils built include a circularly polarized TEM transmit coil with a 32 channel receiver for 7T similar to what is marketed by Nova Medical today, except that ours will fit and operate inside a 33 cm i.d. head gradient coil, and provides a view port with mirror. Another recently successful design includes 32 transceiver loops. A multi-channel, multinuclear ($^{17}\text{O} + ^1\text{H}$) coil is now being tested. These mentioned are but a few diverse examples of a dozen novel head coils that have proven useful for Center studies, 3T-9.4T over the past four years.

Aim 2 to develop the technology required for body imaging at 7T has also been very successful. As for the head in Aim 1, new RF coils and B_1 control systems were designed by computer aided design (CAD) methods, constructed, tested, evaluated and implemented to meet the needs of TRD 4.^{5-9,13,20-23,25,29,33,34} Figures 2–7, and 13-14 give examples of some to the innovative work that has been and is being accomplished in Aim 2 of the present TRD Project 5. Due primarily to transmit efficiency the main coil used today for body imaging at 7T is a pair of transmission line (TEM) arrays including eight elements each for a total of 16 transceiver channels. Success with the multi-channel technologies and B_1 control methods of TRD of Aims 1 and 2 led to the formation of TRD 3, B_1 Field Management in this application.

Aim 3 in the previous funding cycle was to develop technology in support our new 16.4T preclinical system, including system specification, site planning, new probe systems and a multinuclear, multichannel RF front end for this system. This new system was delivered, outfitted per Aim 3, and has been fully operational and productive at the CMRR for the past two years.

Aim 4 was to develop a better understanding of high frequency RF heating and the means to measure it through animal and human modeling, direct measurement in animal models, and ultimately by developing the means to image temperature in humans.^{1,14-19,26,30} “SAR” is considered the primary safety metric in current clinical and research practices. We begin with modeling SAR, but then equate SAR and seven other parameters including the thermal properties of tissues and perfusion to predict temperature, the important safety metric. A new bioheat equation¹ including a term for the dynamic fluctuation of blood perfusate was derived to significantly improve accuracy of temperature prediction. This and all of our numerical models developed in-house are validated with our porcine models in vivo. Thermal imaging using the PRF method has also been performed to achieve relative heating maps with a best resolution of 1 °C. While the “Holy Grail” of imaging the absolute magnitude of thermal contours in the human in vivo, with the needed accuracy and precision of 0.2 °C remains an elusive goal, it will carry over from the present to the new Aims list for the new TRD 5 proposal. The topic of “RF Heating in MRI” was further explored in a recent CMRR - ISMRM hosted workshop, the transactions from which are in press.

Aim 1. Technology for High Field Head, Limb and Animal Imaging

The first aim of TRD Project 5 is concerned with building smaller RF coils for human heads, limbs at 3T, 7T, and 10.5T, and for meeting the preclinical needs of the BTRC at 9.4T and 16.4T. Consistent design themes of these coils are a high count and high spatial distribution of receiver and transceiver channels for best spatial coverage of the region of interest (ROI), for maximizing multi-band and parallel imaging performance, and for reducing SAR. Smaller coil elements will also transmit and receive more uniformly and efficiently (lower radiation resistance) at the frequencies encountered up to 450 MHz (10.5T) and 700 MHz (16.4T) for human and animal coils respectively. While multiple coils will be required for each of 3T, 7T, 9.4T, 10.5T, and 16.4T MRI and NMR systems, the methods for producing them will be similar. For brevity's sake therefore, an



Field / diameter	10.5T/88cm
Manufacturer	Agilent
Temporal Stability	0.03 ppm/hr
Spatial Homogeneity	< 0.07 ppm/25cm dsv
Stored Energy	280 MJ
Conductor	NbTi / 433 km
Temperature	3K
Size	4.1 x 3.2 m
Weight	110 tons
Delivery	October 2011

Figure 10. 10.5T magnet for Center for Magnetic Resonance Research

example of each coil variety will be described and followed through the process of specifying, design, construction, test and evaluation.

As in the Aims, coils are divided into receivers whose function is to receive the NMR signal, transmitters whose function is to excite the NMR signal, and transceivers which both excite and receive. For small coils, particularly those for human studies, we've found that close fitting transmit elements function well as receivers and can be used together with additional receive only elements to further increase the channel count. Therefore we divide the coil circuits into two categories, receive arrays (Aim 1.1) and transceiver arrays (Aim 1.2). A receive array will always be used together with a transceiver array, but not necessarily vice-versa.

Example: 7T Head Coil #1: 3x16 Receiver (3 rings in the z-direction with 16 loops each) with 2x16 Transceiver. (net 80 channel receive x 32 channel transmit) This head coil on order for TRD 1 will be an upgrade of the 3x8 Receive with 1x8 Transceive coil demonstrated in Figure 1. The receiver array for the new coil will be a loop array consisting of three rings of 16 (3x16) decoupled circular loops each, the rings overlapping slightly to critically decouple the mutual inductance between the coil elements in the rings. Figure 11a shows a receive coil comprised of two rings of eight loops each for a simpler, more easily followed example. Each receive includes a decoupling preamp, detuning diode circuits, and a diode based preamp protection circuit. This receiver array will be nested within a transceiver array consisting of two rings of 16 TEM or dipole antenna transceive elements as shown in Figure 11b. The transceiver elements will each include diode detuning, a transmit-receive (TR) switch, and inter-element decoupling by a scheme like in Figure 3. The nested receive and transceiver arrays will then be inserted into a slotted cavity (11c) and packaged with a 3D printed form as shown in Figure 11d. The fabrication work will be performed by Virtumed, LLC, a private company contracted to fabricate our coil designs utilizing rapid prototyping for professional housing design (see examples in Figs. 1 & 13). And yes, through a combination vendor-supplied parallel transmit capability and in-house designed RF front ends, we currently have 32 transmit capability on our 7T actively shielded system. TRD 1 Connectome collaboration funds will pay for this coil. TRD 3 will also benefit by this coil.

Example: 7T Head Coil #2: 3 x16 Transceiver (48 channels receive x 48 channels transmit) Also an extension of a successful 32 channel head coil, this second coil commissioned by TRD 1 will include three rings of 16 transceiver loops, similar in appearance to Figure 11a, but with an extra ring of 16 elements coaxial with the coil. As with the transceiver elements of the first example, each element must be mutually decoupled and will interface a TR switch followed by a preamplifier on the receive port and a power amplifier on the transmit port. All transmit channels in these designs are controlled and driven independently. Except for a limitation on transmit channels, transceiver coils have the significant advantage of reducing the number of coil elements and consequential coil element coupling and shielding in close fitting coils with high element count. This second example coil design will be extended to 4x16 and perhaps higher element counts with the advent of distributed, on-coil power amplifiers to be addressed in Aim 2. This coil also will be supported by the Connectome collaboration. TRD Project 3 will depend on this coil as well.

Example Coil # 3: 3T SWIFT Coil for Head and Knee: In this coil for TRD 2, the material properties of the packaging dictate the design. Protonacious packaging contributes signal in SWIFT sequences.^{73,74} Packaging materials must therefore contain no hydrogen atoms, and/or packaging materials must be shielded from the sample space within the coil. Further the coil requested will be used for human head and knee imaging, and therefore must be open on both ends and split in the "yz" plane so that the top half can be lifted off to better accommodate the knee as well as the head. The simplest, and most certain to perform, first approach to this coil will make use of 16 symmetrically spaced, TEM transceiver elements, with eight elements in each half. This arrangement also facilitates a TRD 2 requirement for simultaneous transmit and receive. The symmetry of this coil allows geometric isolation between transmit and receive, further aided by active isolation feedback and correction pursued in Aim 4 of the TRD Project 5. Once this basic coil is proven successful, additional transceiver channels will be considered. The fabrication costs of \$75k for this initial coil are included in the equipment budget for this proposal.

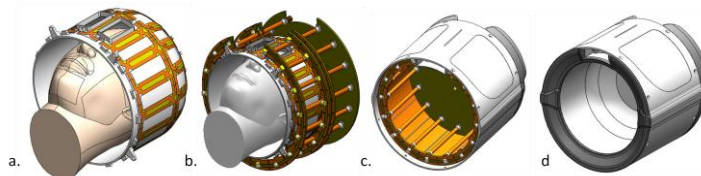


Figure 11. High frequency, "3D" head coil disassembled to show the a) the 32 channel receive elements, b) 32 auto-tuned TEM transceiver elements in x,y,z, c) the slotted, capacitive shield, d) the compact package with view port.

Specification and Design: Head coils for 3T, 7T, 10.5T will be generally built to meet the following criteria. Physical: The i.d. must be 24 cm to snugly fit most human heads (and noses), together with a foam head cup and ear protection. The o.d. will be constrained to 33 cm to fit on top of the patient table, but within optional head gradients. An optical view port will be incorporated into the roof of the coil to permit forward or rear projection screen viewing by means of a configurable mirror. See Figure 11. The coil shall be packaged and connectorized to meet IEC standards. Based on modeling and extrapolation from experience at lower fields, reasonable performance goals are : $B_1 = 0.23 \mu\text{T}/\text{W}^{1/2}$ peak; 15 cm dsv, B_1 shimmed to 80% homogeneity with efficiency = $0.1 \mu\text{T}/\text{W}^{1/2}$; $i\text{SNR} > 165/\mu\text{L}$ in head center; 1.2 mean g-factor for a 4x3 2D reduction factor; decoupling 18dB nominal. SAR = 0.4 W/kg/W.

Construction: To meet these performance specifications the exemplary and additional coils will first be designed in 3D using CAD, built by our Virtumed, LLC partners, and then evaluated prior to delivery by our in-house methods below.

Test and Evaluation: Before a coil or array is put into service, it is rigorously tested, evaluated, and characterized both on the bench and in the magnet. Coil resonance, Q, and isolation, in both the loaded and unloaded condition as well as dynamic detuning are verified on the bench. In the magnet, coil coupling, image homogeneity, transmit efficiency, and SNR are characterized with images from phantoms and then healthy normal volunteers. However, for high-field coils these conventional metrics do not completely characterize the transmit degrees of freedom, spatial characteristics, and the interaction between RF coil fields and imaging methodology. The additional characterization methods required are depicted in Figure 12. The noise covariance matrix⁷⁵ of the loaded array is computed from the collected noise data. B_1^+ shimming calibration data is then acquired.⁷⁶ Individual receiver data is used to calculate receiver sensitivity maps and geometry-factor maps.⁷⁵ The magnitude of the B_1^+ is mapped with two fully-relaxed gradient echo images collected with excitations nominally set to 60° and 120° (double angle method), Figure 12c.⁷⁷ Additionally, the 60° excitation gradient echo image is carefully post-processed so that the result is in SNR units.⁷⁸ Using the B_1 map, the SNR image, and acquisition parameters, the SNR image is converted into intrinsic SNR units which describes receiver performance independent of transmit performance.⁷⁹ By combining the above data, single-channel transmit field maps can be synthesized to predict the transmit efficiency for any B_1^+ shim. The transmit efficiency versus transmit homogeneity can then be calculated for a region and reported for the constraints of 90%, 80%, and 70% transmit homogeneity. Electromagnetic modeling is used to predict the SAR, change in temperature, and an absolute temperature. This coil characterization provides the information needed to predict parallel acceleration performance, transmit efficiency, transmit homogeneity, and the SNR for an arbitrary imaging sequence.

Accordingly, progress toward reaching the stated performance goals can be checked and validated. Furthermore, these results are reported in units that can be compared across systems and field strengths.

Aim 2. Technology for Body Imaging

Two types of body coils will be developed on parallel tracks, 1.) an anterior and posterior pair of body surface coils and 2.) a whole body volume coil. Both will be appropriate for human body imaging at 3T and 7T. The whole body coil will be scalable to 10.5T head imaging.

2.1 Body Surface Coils: The body surface coils are implemented as a pair of nested transmit and receive arrays as pictured in Figure 13, or as a similar pair of transceiver arrays placed anterior and posterior to an ROI in the human subject. A 16 element TEM array with eight channels in each half has proven itself already

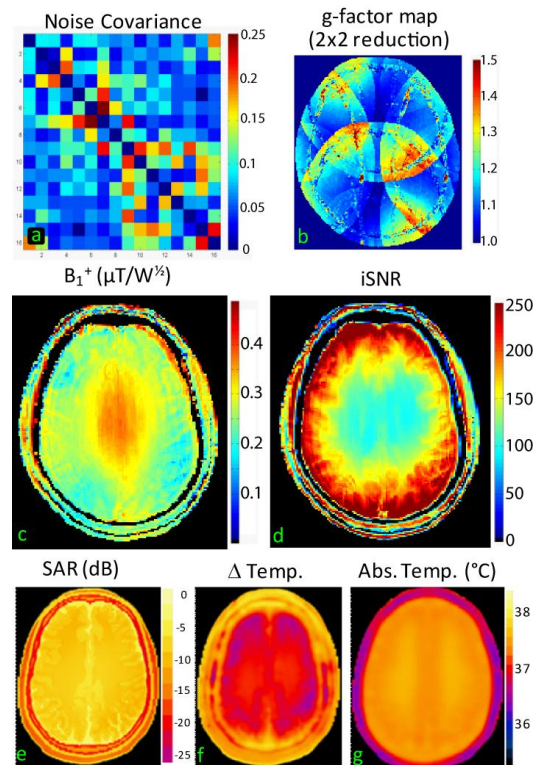


Figure 12. Example coil characterization data of a custom 7T TEM transmit/16 loop receive head coil.

for imaging the heart, kidney, and prostate for TRD 5 and TRD 4.^{63,80,81} To conserve as much as six times more RF power than whole body volume coil, these approaches with body surface coil pairs apply transceiver coil elements arrayed close (5 cm) to the body. The multiple transmit channels facilitate mandatory B_1 shimming of the ROI. Optionally sandwiched between the 16 transceiver elements and the body are receiver arrays which each half with a 2x8 loop array for 32 receive only channels and 16 transceiver channels for a net 48 receive channels. The transmit efficiency, receive sensitivity, and parallel imaging performance of these coils at 7T and higher is moving the field closer to free breathing body imaging, possibly without even cardiac gating. This design will be significantly improved upon by replacing the 32 tuning and matching stems in Figure 13 with electronic or piezoelectric tuning and matching (Figure 5).^{23,82,83} A new upgrade body coil of this design has been requested by TRD Project 4 for body 7T body imaging applications. This new coil will incorporate 32 transceiver elements distributed in a 2x8 per half distribution thus providing multiple rows of transmit elements along Z (referred to in TRD project 3 and 4 as a Z-coil). The Z-coil will include a 32 element receiver also with a 2x8 per half configuration for 32 net transmit channels and 64 receive channels. This coil will be built and evaluated by the methods detailed in Aim 1, and will be fabricated by Virtumed for \$150k.

2.2 Body volume coils: Body volume coils are the standard approach used often together with local receive arrays for clinical imaging applications. See Figure 2, 14a. Typically built into the bore of a magnet, the purpose of the body volume coil is to excite a uniform field over the ROI. With the Larmor frequencies of 3T and above, the B_1 fields generated by conventional body coils become highly nonuniform and the coils become highly inefficient. A different approach is required, and this is what we propose. The traditional monolithic bird cage resonator must become a “multi-channel” coil with a controllable B_1 field for B_1 shimming and multi-band operation. The field must be controllable in three dimensions and so a large number of coil elements must be distributed in x, y, and z dimensions over the surface of the coil cylinder. See Figure 7. Cabling, power, and cost must be conserved by integrating power FETs directly with the coil elements. Bypassing conventional power amplifier combining stages and cables, power losses and therefore costs can be cut by a factor of 3X. See Figure 4, 14b. Automatically tuning these coils per subject will further increase efficiency as shown in Figure 5. Ultimately the whole RF/analog spectrometer will be incorporated into a body coil cylinder inserted into a magnet bore.

Specification and Design: A 48 channel (3x16) TR whole body coil combined with a 32 channel receiver is proposed as shown in Figure 14b. Based on the bore size of the new Siemens SC72 gradients for the new 7T and 10.5T systems, the o.d. of the new body coil must be slightly less than 70 cm. Extrapolating from experience with similar design at 7T (Figure 2, 4), we can set minimum performance specifications to be: peak $B_1 = 0.1 \mu\text{T/W}^{1/2}$; $B_1 = 0.05 \mu\text{T/W}^{1/2}$ for B_1 shimmed to 80% homogeneity over a 15 cm ds; $i\text{SNR} > 70/\mu\text{L}$ in central structures like the prostate for TRD 4. Central slice g-factor = 1.2 for a 6 x 3 2D reduction factor. Coil element decoupling 18 dB nominal. SAR = 0.5 W/kg/W for these specification conditions.

Construction: The 48 channel TEM body transceiver coil depicted in 14b will be designed by TRD 5, fabricated by Virtumed, LLC and evaluated again by the TRD 5 engineers. It will consist of a double sided, slotted cavity



Figure 13. Half of a local, 32 channel receive array is shown next to half of a local, 16 channel transmit array (above). The packaged assembly is shown below.

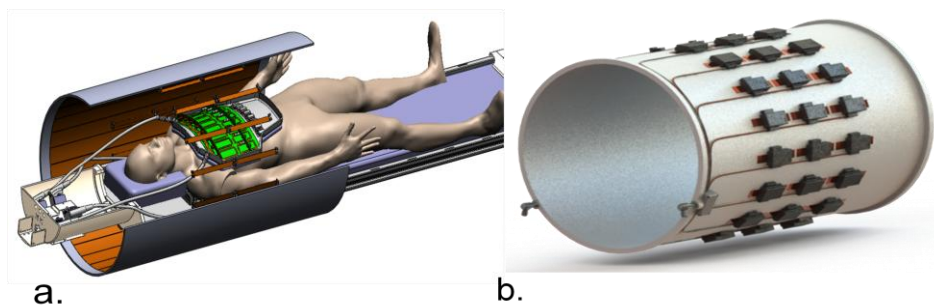


Figure 14. a. High frequency “3D” body coil system comprised of 32-channel transmit and receive elements and a 32-channel loop array within. b. 48 channel (3x16) body coil with 48 distributed power amplifiers on coil.

lining the inside of a fiberglass bore tube of dimensions 65.5 cm x 120 cm. 48, 20 cm long TEM elements will be configured in a 3x16 array. The elements will be staggered and will overlap by 5 cm thereby creating a 50 cm length coil. These elements will be secured to the o.d. of a second, 5 mm wall thickness fiberglass tube of 60 cm o.d. x 120 cm length. 48, 500 W power FETs will be mounted on the 48 coil elements to generate 24 kW peak power at the coil. This would be equivalent to a 48 kW power amplifier in a conventional system plan. The coil elements will serve as heat sinks for the low noise Class E power amplifier modules provided by CPC, Inc. Each of the 48 elements will be auto-tuned as described in Figure 5. The receiver coil planned will be a close fitting pair of 24 element arrays for a combined 48 channel receiver. The full RF body coil system will include 48 transmit channels and 96 receiver channels for best B_1 FOV coverage, 3D B_1 shimming capability, parallel transmit and receive performance and SAR reduction.

The features of this advanced body coil will be scaled to a 16 channel transceive head coil with a 2x8 element configuration, on-coil amplifiers, and auto-tuning and matching. The coil will be built as an engineering test-bed for evaluation at both 7T and 10.5T.

Test and Evaluation: T&E will proceed as described for the head coils in Specific Aim 1. A similar basic coil system (though far less sophisticated) has been demonstrated to be successful at 7T (Figure 2). Fabrication costs for these advanced head and body volume coils will cost a total \$225k.

Aim 3. RF Coil Interface and Control Circuits

New RF coil technologies require, or could greatly benefit from new MRI system interface and control circuits. Four such interface circuit developments are planned or currently underway.

3.1 Auto-tune and match: Currently multi-channel transmit, receive, and transceiver coils are operated with fixed tuned frequencies and impedance match positions. This approach virtually guarantees that coils will be poorly tuned and matched for most conditions; the consequences are lower power transmit efficiency and lower receive sensitivity. We are currently working on two approaches to automatically tune and match a coil to its load conditions. One approach uses negative feedback to drive nonmagnetic piezoelectric motors to actuate tuning and matching stubs in individual transmit coil elements. The other approach uses PIN diode switching of capacitance matrices for tune and match functions. This innovative approach is highlighted in Figure 5 above. Both approaches will be pursued until one proves more satisfactory.

3.2 On-coil power amps: On most commercial systems, RF power amplifiers are housed in large cabinets located in a equipment room typically remote from the magnet. In very common solid-state amplifiers, power FETs must be combined to board and stage level. This combining is often inefficient and distorts the signal, costing as much as 1/3 the power and diminished phase and gain linearity. Moving the amplified signal from the power amp to the coil over forty feet of RG 214 or heavier cable typically costs additional signal instabilities and another 1/3 of the original power FET output. Both of these sources of loss totaling 2/3 of the power output of power FETs will be eliminated by our development of nonmagnetic power amps that will be distributed over the elements of a transmit or transceive multi-channel coil. Additionally removing the cable bulk required will make transmit coils with large element counts practical.

3.3 On-coil monitoring: Integral with feedback driven auto-tuning and matching, feedback driven on-coil power amp signal corrections, and RF safety is the monitoring of the RF signal on each and every independent coil element. In-line, forward and reverse coupling of a small signal RF coupling at the coil and inductive coupling of the RF field generated by each coil element are two means by which to monitor the RF signal at the coil. These means will be developed in concert with Aims 3.1 and 3.2 above and Aim 5 below.

Aim 4. New RF Concepts

4.1 SWIFT circuits: Three contributions to improve technology in support of SWIFT MRI in TRD Project 2 are proposed, the on-coil transceiver SWIFT compatible coils and a simultaneous transmit and receive circuit. The analog integrated transceiver circuit is described in Figure 6 and the coil is described in the plan for Aim 1, example 3. Simultaneous transmit and receive is an important concept to be developed in TRD 2. We will support the technology need for this development by a two step approach. Step 1 will enhance the already demonstrated separation of transmit and receive signals by a 90° phase shift, by broadening and stabilizing this quadrature isolation with baluns in the transmit and receive legs.⁸⁴ A more challenging but ultimately higher precision Step 2 will make use of a dynamic, feedback driven isolation correction routine which will automatically and continuously correct for load swings to maintain a 90° TR separation. This will be accomplished by the same approach as our automatic tuning and matching of Figure 5 and Aim 3.

4.2 Dielectrics for RF lensing and impedance matching: In addition to supporting TRD Project 3 with extensive development of multi-channel coils, parallel transceivers and other technologies required to facilitate B_1 field management, TRD 5 will investigate material and geometric options for RF field profiling and coil-sample impedance matching. These options will be rapidly and comprehensively explored through numerical simulations and prototyping of the most promising results.

4.3 Local shims, gradients, and RF coils: B_0 field homogeneity as well as B_1 uniformity affects image quality. Dr. de Graaf of Yale has developed a novel B_0 shimming coil and technique for the human brain based on the combination of non orthogonal basis fields from 48 individual circular shim coils. Custom built amplifiers allowed for dynamic control of the multi-channel shim coil field that was fast and precise enough to mimic slice selection gradients, and with 48 degrees of freedom, able to correct for steep susceptibility gradient artifacts.⁸⁵⁻⁸⁷ This dynamic, multi-coil shimming has significantly improved B_0 homogeneity of the brain at 7T. Through collaboration we will interface our close fitting, multi-channel RF head coils with Yale's close fitting, 48 channel head shim coils for dynamic control with best performance for B_0 and B_1 dependent parameters for TRD 1's brain applications.

Aim 5. RF Safety

The primary purpose of this Aim is to assure human safety in the studies proposed in the BTRC and collaborations. In addition the practical need for safety data for new technologies, new methods and new unprecedented field strengths will also be answered by this accomplishing Aim 5. Local SAR and temperature contours will be numerically predicted using digitized porcine and human models for whole bodies. Systemic and local temperature predictions will be validated in direct measurements in anesthetized pigs, in vivo. Measured temperature in pigs will be correlated to measured input power using the same coils, amplifiers, and protocols proposed herein for human use. In addition to publishing the data acquired from these studies, it will be submitted to the FDA and to our IRB in annual progress reports.

5.1 SAR and temperature modeling: SAR and temperature will be predicted in our porcine models (Figure 9) by calculating power loss density (SAR) for given coils, frequencies and power settings. Temperature will then be equated to SAR by our bioheat equation including terms for the electro-dynamics, thermodynamics, and physiology of the model.

In our RF Safety Collaboration, systemic and local temperature predictions will be validated by direct measurements in anesthetized pigs, in vivo. Measured temperature in pigs will be correlated to measured input power using the same coils, amplifiers and protocols proposed herein for human use. RF coils used for these measurements will be

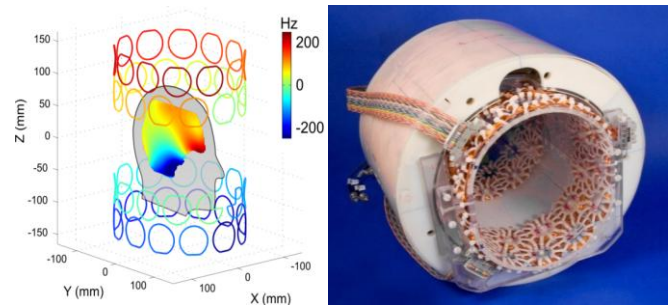
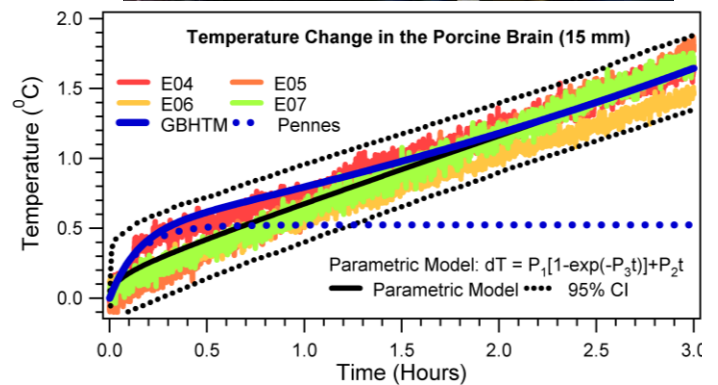
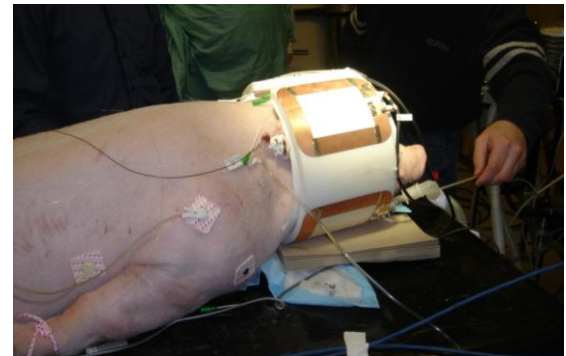


Figure 15. 48 channel B_0 + 8 channel B_1 Coil. B_0 shim coils diagrammed (left) are integrated with RF (right).



$$(\rho C_p)_T \frac{\partial \langle T \rangle^T}{\partial t} = G_1 (\nabla \cdot k_T \nabla \langle T \rangle^T) + \frac{US_{T-BI}}{V(1-\epsilon)} (\langle T \rangle^{BI} - \langle T \rangle^T) + \langle Q \rangle^T$$

(Transient Term) (Conduction Term) (Blood-Tissue Heat Transfer Rate Term) (Source Term)

Figure 16. Photo shows setup for direct measurement of RF heating. The resulting temperature versus time data is plotted together with fits from the classic bio-heat equation (Pennes – dotted blue line) and our Generic Bioheat equation (solid blue line), shown in the equation^{1,2}.

characterized in terms of °C/W/kg. Temperature will be measured on the modeled coronal, axial, and sagittal planes, rectally, and also adjacent to receiver coils placed on the porcine model within the head and body coils. In this way any power coupled to receiver loops will be monitored for local heating, in addition to the measured core heating. Figure 16 illustrates the technique of fiber optic probe placement in a pig within a coil field.

5.2 RF safety protocol implementation: To assure human safety in the planned investigations, system power monitors will be set using either 1.) FDA SAR guideline limits for head or body, or 2.) measured SAR values correlated to FDA temperature guideline limits, whichever is the lower value. In this manner, we will be more certain of compliance and safety. RF power will be monitored per channel in multi-channel transceiver coils. A priori information determined from the SAR and temperature modeling and measurement components of this proposal will be used to establish and set RF power limits, per coil, load, and power setting for a given experiment. Forward and reverse power will be monitored per channel. Each channel will be independently limited. Additionally power will be integrated for all channels. In this way, both local and global power will be monitored. When any preset limit is exceeded on single or multiple elements, a redundant failsafe will both blank RF power to the parallel transceiver, and will power off each power amplifier of the parallel transceiver.

5.3 Development of new RF safety protocol: Based on the understanding that individual specific temperature profiles and not a one-size-fits-all SAR limit is the correct approach to RF safety assurance, a new pre-scan safety protocol is proposed. Following the flow chart diagramed in Figure 17, first a patient would be rapidly scanned from head to toe, or the range appropriate to a local coil, with a moving table. The resulting 3D data set would then be segmented into at least two tissue types, 1.) high water content, high conductivity tissue, and 2.) low water content, low conductivity tissue. Tissue segments will next be assigned table values for conductivity and permittivity. Additional information about the patient would be entered into this routine, including coil specifics, scan pulse protocol, and patient specifics such as weight, disease, anesthesia, implants, perfusion constrictors, heart rate, blood pressure, respiratory rate, temperature, blankets, and other data that may affect temperature. Considering this data, a temperature map would then be calculated for this specific patient and scan protocol. Predictions of excessive temperature in local hot spots or global hyperthermia would be grounds for cancelling or modifying the scan. All of these operations would need to be completed within five minutes. We have proven the feasibility of this approach with pig models (Figure 9) and human models (Figure 8) over longer periods of time and off-line to the MRI system. The main goal of this aim therefore would be to perform this thermal prescan at the console in under five minutes. A hybrid analytical/method of moments approach is being considered for the calculation speed required.

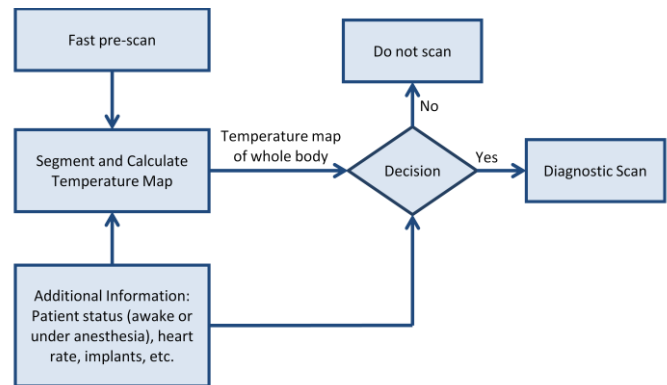


Figure 17. Flow chart for RF safety pre-scan protocol.

Considering this data, a temperature map would then be calculated for this specific patient and scan protocol. Predictions of excessive temperature in local hot spots or global hyperthermia would be grounds for cancelling or modifying the scan. All of these operations would need to be completed within five minutes. We have proven the feasibility of this approach with pig models (Figure 9) and human models (Figure 8) over longer periods of time and off-line to the MRI system. The main goal of this aim therefore would be to perform this thermal prescan at the console in under five minutes. A hybrid analytical/method of moments approach is being considered for the calculation speed required.

5.4 NMR Thermometry: Imaging temperature contours has long been considered the “Holy Grail” for RF heating determination. The proton resonance frequency (PRF) shift method has been demonstrated the most successful approach to date. This approach however does not achieve the 0.2 °C accuracy and precision required to measure temperature for safety purposes. For our pig model at least, we can improve on the PRF approach by introducing exogenous Tm-based macrocyclic complexes, such as TmDOTA⁻, which have showed 100 times greater sensitivity to temperature than water proton frequency shifts.⁸⁸⁻⁹³ The feasibility of imaging absolute temperature with a paramagnetic lanthanide complex using water as a reference has been demonstrated in rodents.⁹¹ The rodents were thermally stable and therefore imaging time was unconstrained. To be applicable for RF heating studies, this methodology must be adapted to either imaging of RF heating in the steady state, and/or acquisition acceleration. Development of this methodology for imaging RF heating in phantoms is proposed. Once developed, it will be available to Collaborative Project 10 for imaging of RF heating in live pig studies. This approach will take us one step closer to thermal imaging of humans.

E. REFERENCES

1. Shrivastava, D. & Vaughan, J. T. *A generic bioheat transfer thermal model for a perfused tissue*. (2009) *J Biomech Eng* **131**, 074506.
2. Adriany, G., Van de Moortele, P.-F., Ritter, J., Voje, W., Vaughan, J. T. & Ugurbil, K., *Spatially reconfigurable magnetic resonance coil* (Patent) 2009 Issuing Organization: USPTO.
3. Adriany, G. in *Encyclopedia of Magnetic Resonance* *Published on line before Print DOI: 10.1002/9780470034590.emrstm1096* (ed R. K. Harris and R. E. Wasylishen) (John Wiley & Sons, Ltd., Chichester, 2012).
4. Adriany, G., Auerbach, E. J., Snyder, C. J., Gozubuyuk, A., Moeller, S., Ritter, J., Van de Moortele, P. F., Vaughan, T. & Ugurbil, K. *A 32-channel lattice transmission line array for parallel transmit and receive MRI at 7 tesla*. (2010) *Magn Reson Med* **63**, 1478-1485.
5. Akgun, C. E., Snyder, C., DelaBarre, L., Moeller, S., Van de Moortele, P. F., Vaughan, J. T. & Ugurbil, K., *Three Dimensional RF Coil Structures for Field Profiling*. (Patent) 2009. Issuing Organization: USPTO, Published Source: USPTO.
6. Akgun, C. E. *Radiofrequency Fields and SAR for Tranverse Electromagnetic (TEM) Surface Coils*. (2012) in "RF Coils for MRI", pages 387-396; eds J. T. Vaughan & J. R. Griffiths. *Series Vol. Chapter 30* (John Wiley).
7. Akgun, C. E., DelaBarre, L., Yoo, H., Sohn, S.-M., Snyder, C. J., Adriany, G., Ugurbil, K., Gopinath, A. & Vaughan, J. T. *Stepped Impedance Resonators for High Field Magnetic Resonance Imaging*. (2012) *Transactions on Biomedical Engineering* In Press.
8. Metzger, G. J., Auerbach, E. J., Akgun, C., Simonson, J., Bi, X., Ugurbil, K. & van de Moortele, P. F. *Dynamically Applied B1+ Shimming Solutions for Non-Contrast Enhanced Renal Angiography at 7.0 Tesla*. (2012) *Magn Reson Med* In Press.
9. Metzger, G. J., van de Moortele, P. F., Akgun, C., Snyder, C. J., Moeller, S., Strupp, J., Andersen, P., Shrivastava, D., Vaughan, T., Ugurbil, K. & Adriany, G. *Performance of external and internal coil configurations for prostate investigations at 7 T*. (2010) *Magn Reson Med* **64**, 1625-1639.
10. Olson, C., Yoo, H., DelaBarre, L. & Vaughan, J. *RF B1 field localization through convex optimization*. (2012) *Optical Technology Letters* **54**.
11. Olson, C. C., Vaughan, J. T. & Gopinath, A., *Radio frequency field localization for magnetic resonance* (Patent) 2009. Issuing Organization: USPTO Patent Number: 7,633,293.
12. Omar, A., Caverly, R., Doherty, W. E., Watkins, R., Gopinath, A. & Vaughan, J. T. **A Microwave Engineer's View of MRI**. (2011) *IEEE Microwave Magazine* **12**, 78-86.
13. Schmitter, S., Auerbach, E. J., Adriany, G., Ugurbil, K. & Van de Moortele, P. F. *Towards clinical application of 7T TOF angiography*. (2012) *J Cardiovasc Magn Reson* **14 Suppl 1**, W72.
14. Shrivastava, D., Abosch, A., Hanson, T., Tian, J., Gupte, A., Iaiizzo, P. A. & Vaughan, J. T. *Effect of the extracranial deep brain stimulation lead on radiofrequency heating at 9.4 Tesla (400.2 MHz)*. (2010) *J Magn Reson Imaging* **32**, 600-607.
15. Shrivastava, D., Goerke, U., Porter, D. & Vaughan, J. T. *New Developments in Bioheat Transfer Modeling and MR Thermometry to Improve Radiofrequency Safety in High Field Field MRI*. (2012) in "RF Safety for MRI", pages In Press; eds J. T. Vaughan & D. Shrivastava. *Series Vol. Chapter 13* (International Society for Magnetic Resonance in Medicine).
16. Shrivastava, D., Gordon, C. J. & Vaughan, J. T. *Selective Brain Cooling in Humans during Exercise*. (2011) *Journal of Applied Physiology* **110**, 580-580.
17. Shrivastava, D., Hanson, T., Kulesa, J., DelaBarre, L., Iaiizzo, P. & Vaughan, J. T. *Radio frequency heating at 9.4T (400.2 MHz): in vivo thermoregulatory temperature response in swine*. (2009) *Magn Reson Med* **62**, 888-895.
18. Shrivastava, D., Hanson, T., Kulesa, J., Tian, J., Adriany, G. & Vaughan, J. T. *Radiofrequency heating in porcine models with a "large" 32 cm internal diameter, 7 T (296 MHz) head coil*. (2011) *Magn Reson Med* **66**, 255-263.
19. Shrivastava, D. & Vaughan, J. T. *Radiofrequency Heating Measurements and Models*. (2012) in "RF Coils for MRI", pages 425-436; eds J. T. Vaughan & J. R. Griffiths. *Series Vol. Chapter 33* (John Wiley).
20. Snyder, C. *TEM Arrays, Design and Implementation*. (2012) in "RF Coils for MRI", pages 169-174; eds J. T. Vaughan & J. R. Griffiths. *Series Vol. Chapter 14* (John Wiley).

21. Snyder, C. J., DelaBarre, L., Metzger, G. J., van de Moortele, P. F., Akgun, C., Ugurbil, K. & Vaughan, J. T. *Initial results of cardiac imaging at 7 Tesla*. (2009) *Magn Reson Med* **61**, 517-524.
22. Snyder, C. J., Delabarre, L., Moeller, S., Tian, J., Akgun, C., Van de Moortele, P. F., Bolan, P. J., Ugurbil, K., Vaughan, J. T. & Metzger, G. J. *Comparison between eight- and sixteen-channel TEM transceive arrays for body imaging at 7 T*. (2012) *Magn Reson Med* **67**, 954-964.
23. Snyder, C. J. & Vaughan, J. T., *Remotely adjustable reactive and resistive electrical element and method*. *Appl. 61/158345* (Patent) 2009. Issuing Organization: USPTO.
24. Sohn, S.-M., Vaughan, J. & Gopinath, A. *An interdigitated split-ring resonator for meta materials*. (2011) *Microwave and Optical Technology Letters* **53**, 4.
25. Suttie, J. J., Delabarre, L., Pitcher, A., van de Moortele, P. F., Dass, S., Snyder, C. J., Francis, J. M., Metzger, G. J., Weale, P., Ugurbil, K., Neubauer, S., Robson, M. & Vaughan, T. *7 Tesla (T) human cardiovascular magnetic resonance imaging using FLASH and SSFP to assess cardiac function: validation against 1.5 T and 3 T*. (2012) *NMR in Biomedicine* **25**, 27-34.
26. Tian, J. *TEM Fields and SAR*. (2012) in "RF Coils for MRI", pages 397-406; eds J. T. Vaughan & J. R. Griffiths. *Series Vol. Chapter 31* (John Wiley).
27. Vaughan, J. & Tian, J., *Coil Element Decoupling for MRI*. (Patent) 2012. Issuing Organization: USPTO, Published Source: USPTO.
28. Vaughan, J. T., *RF Coil for Imaging Systems and Methods of Operation*. (Patent) 2009. Issuing Organization: USPTO Patent Number: US 2009/0237077 A1.
29. Vaughan, J. T. *TEM Body Coils*. (2012) in "RF Coils for MRI", pages 147-167; eds J. T. Vaughan & J. R. Griffiths. *Series Vol. Chapter 13* (John Wiley).
30. Vaughan, J. T. *RF Coil Heating and Mitigation*. (2012) in "RF Safety for MRI", pages In Press; eds J. T. Vaughan & D. Shrivastava. *Series Vol. Chapter 20* (International Society for Magnetic Resonance in Medicine).
31. Vaughan, J. T., Adriany, G., Snyder, C., Akgun, C. E., Tian, J., Ugurbil, K., Van de Moortele, P.-F. & Moeller, S., *Multi-current elements for magnetic resonance radio frequency coils* (Patent) 2010. Issuing Organization: USPTO Patent Number: 7,710,117.
32. Vaughan, J. T., Adriany, G. & Ugurbil, K., *Assymmetric radio frequency magnetic line array* (Patent) 2011. Issuing Organization: USPTO.
33. Vaughan, J. T., Snyder, C. J., DelaBarre, L. J., Bolan, P. J., Tian, J., Bolinger, L., Adriany, G., Andersen, P., Strupp, J. & Ugurbil, K. *Whole-body imaging at 7T: preliminary results*. (2009) *Magn Reson Med* **61**, 244-248.
34. Vaughan, J. T., Ugurbil, K. & Adriany, G., *Radio frequency gradient, shim and parallel imaging coil*. (Patent) 2009. Issuing Organization: USPTO.
35. Vaughan, J. T., Van de Moortele, P.-F., DelaBarre, L., Olson, C. C., Orser, H., Gopinath, A., Ugurbil, K., Snyder, C., Adiany, G., Akgun, C. E., Tian, J., Strupp, J., Andersen, P. M. & Wu, X., *High field magnetic resonance* (Patent) 2010. Issuing Organization: USPTO Patent Number: 7,800,368.
36. Wu, X., Akgun, C., Vaughan, J. T., Andersen, P., Strupp, J., Ugurbil, K. & Van de Moortele, P. F. *Adapted RF pulse design for SAR reduction in parallel excitation with experimental verification at 9.4 T*. (2010) *J Magn Reson* **205**, 161-170.
37. Wu, X., Vaughan, J. T., Ugurbil, K. & Van de Moortele, P. F. *Parallel excitation in the human brain at 9.4 T counteracting k-space errors with RF pulse design*. (2010) *Magn Reson Med* **63**, 524-529.
38. Yoo, H., Vaughan, J. T. & Gopinath, A. *RF (B_1) Field Calculation with Transmission Line Resonator Analysis for High-Field Magnetic Resonance Systems*. (2011) *IEEE Antennas and Wireless Propagation Letters* **10**.
39. Zhang, X., Van de Moortele, P. F., Schmitter, S. & He, B. *Complex B_1 Mapping and Electrical Properties Imaging of the Human Brain using a 16-channel Transceiver Coil at 7T*. (2012) *Magn Reson Med* **In Press**.
40. Vaughan, J. T., Garwood, M., Collins, C. M., Liu, W., DelaBarre, L., Adriany, G., Andersen, P., Merkle, H., Goebel, R., Smith, M. B. & Ugurbil, K. *7T vs. 4T: RF power, homogeneity, and signal-to-noise comparison in head images*. (2001) *Magnetic Resonance in Medicine* **46**, 24-30.
41. Vaughan, T., DelaBarre, L., Snyder, C., Tian, J., Akgun, C., Shrivastava, D., Liu, W., Olson, C., Adriany, G., Strupp, J., Andersen, P., Gopinath, A., van de Moortele, P. F., Garwood, M. & Ugurbil, K. *9.4T human MRI: preliminary results*. (2006) *Magnetic Resonance in Medicine* **56**, 1274-1282.

42. Rooney, W. D., Johnson, G., Li, X., Cohen, E. R., Kim, S. G., Ugurbil, K. & Springer, C. S., Jr. *Magnetic field and tissue dependencies of human brain longitudinal 1H2O relaxation in vivo*. (2007) *Magnetic Resonance in Medicine* **57**, 308-318.
43. Yacoub, E., Harel, N. & Ugurbil, K. *High-field fMRI unveils orientation columns in humans*. (2008) *Proc Natl Acad Sci U S A* **105**, 10607-10612.
44. Yacoub, E., Shmuel, A., Pfeuffer, J., Van De Moortele, P. F., Adriany, G., Andersen, P., Vaughan, J. T., Merkle, H., Ugurbil, K. & Hu, X. *Imaging brain function in humans at 7 Tesla*. (2001) *Magnetic Resonance in Medicine* **45**, 588-594.
45. Yacoub, E., Shmuel, A., Pfeuffer, J., Van De Moortele, P. F., Adriany, G., Ugurbil, K. & Hu, X. *Investigation of the initial dip in fMRI at 7 Tesla*. (2001) *NMR in Biomedicine* **14**, 408-412.
46. Duong, T. Q., Yacoub, E., Adriany, G., Hu, X. P., Ugurbil, K., Vaughan, J. T., Merkle, H. & Kim, S. G. *High-resolution, spin-echo BOLD, and CBF AM at 4 and 7 T*. (2002) *Magnetic Resonance in Medicine* **48**, 589-593.
47. Pfeuffer, J., Adriany, G., Shmuel, A., Yacoub, E., Van De Moortele, P. F., Hu, X. & Ugurbil, K. *Perfusion-based high-resolution functional imaging in the human brain at 7 Tesla*. (2002) *Magnetic Resonance in Medicine* **47**, 903-911.
48. Pfeuffer, J., van de Moortele, P. F., Yacoub, E., Shmuel, A., Adriany, G., Andersen, P., Merkle, H., Garwood, M., Ugurbil, K. & Hu, X. *Zoomed functional imaging in the human brain at 7 Tesla with simultaneous high spatial and high temporal resolution*. (2002) *Neuroimage* **17**, 272-286.
49. Shmuel, A., Yacoub, E., Pfeuffer, J., Van de Moortele, P. F., Adriany, G., Hu, X. & Ugurbil, K. *Sustained negative BOLD, blood flow and oxygen consumption response and its coupling to the positive response in the human brain*. (2002) *Neuron* **36**, 1195-1210.
50. Duong, T. Q., Yacoub, E., Adriany, G., Hu, X., Ugurbil, K. & Kim, S. G. *Microvascular BOLD contribution at 4 and 7 T in the human brain: gradient-echo and spin-echo fMRI with suppression of blood effects*. (2003) *Magnetic Resonance in Medicine* **49**, 1019-1027.
51. Yacoub, E., Duong, T. Q., Van De Moortele, P. F., Lindquist, M., Adriany, G., Kim, S. G., Ugurbil, K. & Hu, X. *Spin-echo fMRI in humans using high spatial resolutions and high magnetic fields*. (2003) *Magnetic Resonance in Medicine* **49**, 655-664.
52. Duong, T. Q., Yacoub, E., Adriany, G., Hu, X. P., Andersen, P., Vaughan, J. T., Ugurbil, K. & Kim, S. G. *Spatial specificity of high-resolution, spin-echo BOLD, and CBF fMRI at 7 T*. (2004) *Magnetic Resonance in Medicine* **51**, 646-647.
53. Shmuel, A., Yacoub, E., Chaimow, D., Logothetis, N. K. & Ugurbil, K. *Spatio-temporal point-spread function of fMRI signal in human gray matter at 7 Tesla*. (2007) *Neuroimage* **35**, 539-552.
54. Yacoub, E., Van De Moortele, P. F., Shmuel, A. & Ugurbil, K. *Signal and noise characteristics of Hahn SE and GE BOLD fMRI at 7 T in humans*. (2005) *Neuroimage* **24**, 738-750.
55. Yacoub, E., Shmuel, A., Logothetis, N. & Ugurbil, K. *Robust detection of ocular dominance columns in humans using Hahn Spin Echo BOLD functional MRI at 7 Tesla*. (2007) *Neuroimage* **37**, 1161-1177.
56. Tkac, I., Andersen, P., Adriany, G., Merkle, H., Ugurbil, K. & Gruetter, R. *In vivo 1H NMR spectroscopy of the human brain at 7 T*. (2001) *Magnetic Resonance in Medicine* **46**, 451-456.
57. Mangia, S., Tkac, I., Gruetter, R., Van De Moortele, P. F., Giove, F., Maraviglia, B. & Ugurbil, K. *Sensitivity of single-voxel 1H-MRS in investigating the metabolism of the activated human visual cortex at 7 T*. (2006) *Magnetic Resonance Imaging* **24**, 343-348.
58. Mangia, S., Tkac, I., Gruetter, R., Van de Moortele, P. F., Maraviglia, B. & Ugurbil, K. *Sustained neuronal activation raises oxidative metabolism to a new steady-state level: evidence from 1H NMR spectroscopy in the human visual cortex*. (2007) *J Cereb Blood Flow Metab* **27**, 1055-1063.
59. Mangia, S., Tkac, I., Logothetis, N. K., Gruetter, R., Van de Moortele, P. F. & Ugurbil, K. *Dynamics of lactate concentration and blood oxygen level-dependent effect in the human visual cortex during repeated identical stimuli*. (2007) *J Neurosci Res* **85**, 3340-3346.
60. Wiesinger, F., Van De Moortele, P. F., Adriany, G., De Zanche, N., Ugurbil, K. & Pruessmann, K. P. *Parallel imaging performance as a function of field strength - An experimental investigation using electrodynamic scaling*. (2004) *Magnetic Resonance in Medicine* **52**, 953-964.
61. Wiesinger, F., Van de Moortele, P. F., Adriany, G., De Zanche, N., Ugurbil, K. & Pruessmann, K. P. *Potential and feasibility of parallel MRI at high field*. (2006) *NMR in Biomedicine* **19**, 368-378.

62. Moeller, S., Van de Moortele, P. F., Goerke, U., Adriany, G. & Ugurbil, K. *Application of parallel imaging to fMRI at 7 Tesla utilizing a high 1D reduction factor.* (2006) *Magnetic Resonance in Medicine* **56**, 118-129.
63. Snyder, C. J., DelaBarre, L., Metzger, G. J., van de Moortele, P. F., Akgun, C., Ugurbil, K. & Vaughan, J. T. *Initial results of cardiac imaging at 7 Tesla.* (2009) *Magnetic Resonance in Medicine* **61**, 517-524.
64. Vaughan, T., Snyder, C., DelaBarre, L., Bolinger, L., Tian, J., Andersen, P., Strupp, J., Adriany, G. & Ugurbil, K. *7T Body Imaging: First Results.* Proceedings 14th Scientific Meeting, International Society for Magnetic Resonance in Medicine; May; Seattle, WA2006. p. 213.
65. Shrivastava, D., Hanson, T., Schlentz, R., Gallagher, W., Snyder, C., Delabarre, L., Prakash, S., Iaizzo, P. & Vaughan, J. T. *Radiofrequency heating at 9.4T: in vivo temperature measurement results in swine.* (2008) *Magnetic Resonance in Medicine* **59**, 73-78.
66. Shrivastava, D., Hanson, T., Kulesa, J., Tian, J., Adriany, G. & Vaughan, J. T. *Radiofrequency heating in porcine models with a "large" 32 cm internal diameter, 7 T (296 MHz) head coil.* (2011) *Magnetic Resonance in Medicine* **66**, 255-263.
67. Adriany, G., Auerbach, E. J., Snyder, C. J., Gozubuyuk, A., Moeller, S., Ritter, J., Van de Moortele, P. F., Vaughan, T. & Ugurbil, K. *A 32-channel lattice transmission line array for parallel transmit and receive MRI at 7 tesla.* (2010) *Magnetic Resonance in Medicine* **63**, 1478-1485.
68. Adriany, G., Gozubuyuk, A., Auerbach, E. J., Van de Moortele, P. F., Andersen, P., Moeller, S., Vaughan, J. T. & Ugurbil, K. *A 32 channel Transmit/Receive Transmission Line Head Array for 3D RF Shimming.* ISMRM; Berlin, Germany2007. p. 168.
69. SEMCAD. *Reference Manual for the SEMCAD X Simulation Platform for Electromagnetic compatibility, antenna design, and dosimetry. Version 11.0.* (2006).
70. Shrivastava, D. & Vaughan, J. T. *Development of an Anatomically Accurate Porcine Head Model to Study Radiofrequency Heating due to MRI.* Proceedings 18th Scientific Meeting, International Society for Magnetic Resonance in Medicine; Stockholm, Sweeden2010.
71. Dewhirst, M. W., Viglianti, B. L., Lora-Michiels, M., Hanson, M. & Hoopes, P. J. *Basic principles of thermal dosimetry and thermal thresholds for tissue damage from hyperthermia.* (2003) *Int J Hyperthermia* **19**, 267-294.
72. Schmitter, S., Auerbach, E. J., Adriany, G., Ugurbil, K. & Van de Moortele, P.-F. *Towards clinical application of 7T TOF angiography.* (2012) *Journal of Cardiovascular Magnetic Resonance* **14**, W72.
73. Idiyatullin, D., Corum, C., Park, J. Y. & Garwood, M. *Fast and quiet MRI using a swept radiofrequency.* (2006) *Journal of Magnetic Resonance* **181**, 342-349.
74. Marjanska, M., Waks, M., Snyder, C. J. & Vaughan, J. T. *Multinuclear NMR investigation of probe construction materials at 9.4T.* (2008) *Magnetic Resonance in Medicine* **59**, 936-938.
75. Pruessmann, K. P., Weiger, M., Scheidegger, M. B. & Boesiger, P. *SENSE: sensitivity encoding for fast MRI.* (1999) *Magnetic Resonance in Medicine* **42**, 952-962.
76. Van de Moortele, P. F., Akgun, C., Adriany, G., Moeller, S., Ritter, J., Collins, C. M., Smith, M. B., Vaughan, J. T. & Ugurbil, K. *B₁ destructive interferences and spatial phase patterns at 7 T with a head transceiver array coil.* (2005) *Magnetic Resonance in Medicine* **54**, 1503-1518.
77. Insko, E. & Bolinger, L. *Mapping of the Radiofrequency Field", JMR Series A, 102, 82-85 (1993).* (1993) *Journal of Magnetic Resonance. Series A* **102**, 82-85.
78. Kellman, P. & McVeigh, E. R. *Image reconstruction in SNR units: a general method for SNR measurement.* (2005) *Magnetic Resonance in Medicine* **54**, 1439-1447.
79. Adriany, G., Van de Moortele, P. F., Wiesinger, F., Moeller, S., Strupp, J. P., Andersen, P., Snyder, C., Zhang, X., Chen, W., Pruessmann, K. P., Boesiger, P., Vaughan, T. & Ugurbil, K. *Transmit and receive transmission line arrays for 7 Tesla parallel imaging.* (2005) *Magnetic Resonance in Medicine* **53**, 434-445.
80. Metzger, G. J., Snyder, C., Akgun, C., Vaughan, T., Ugurbil, K. & Van de Moortele, P. F. *Local B₁₊ shimming for prostate imaging with transceiver arrays at 7T based on subject-dependent transmit phase measurements.* (2008) *Magnetic Resonance in Medicine* **59**, 396-409.
81. Snyder, C. J., Delabarre, L., Moeller, S., Tian, J., Akgun, C., Van de Moortele, P. F., Bolan, P. J., Ugurbil, K., Vaughan, J. T. & Metzger, G. J. *Comparison between eight- and sixteen-channel TEM transceive arrays for body imaging at 7 T.* (2012) *Magnetic Resonance in Medicine* **67**, 954-964.

82. Snyder, C., DelaBarre, L., Tian, J., Akgun, C. & Vaughan, J. T. Using Piezoelectric Actuators for Remote Tuning of Transmit Coils. In: Proceedings of the 19th Annual Meeting of ISMRM; Stockholm2010. p. 1523.
83. Snyder, C., Rogers, C., DelaBarre, L., Robson, M. & Vaughan, J. T. in *Proceedings of the 19th Annual Meeting of ISMRM*, (Montreal, Quebec, 2011).
84. Idiyatullin, D., Suddarth, S., Corum, C., Adriany, G. & Garwood, M. *Continuous SWIFT*. (2011) Proc Intl Soc Magn Reson Med **19**, 382.
85. Juchem, C., Brown, P. B., Nixon, T. W., McIntyre, S., Rothman, D. L. & de Graaf, R. A. *Multicoil shimming of the mouse brain*. (2011) Magnetic Resonance in Medicine **66**, 893-900.
86. Juchem, C., Nixon, T. W., Diduch, P., Rothman, D. L., Starewicz, P. & De Graaf, R. A. *Dynamic Shimming of the Human Brain at 7 Tesla*. (2010) Concepts Magn Reson Part B Magn Reson Eng **37B**, 116-128.
87. Juchem, C., Nixon, T. W., McIntyre, S., Rothman, D. L. & de Graaf, R. A. *Magnetic field homogenization of the human prefrontal cortex with a set of localized electrical coils*. (2010) Magnetic Resonance in Medicine **63**, 171-180.
88. Hekmatyar, S. K., Poptani, H., Babsky, A., Leeper, D. B. & Bansal, N. *Non-invasive magnetic resonance thermometry using thulium-1,4,7,10-tetraazacyclododecane-1,4,7,10-tetraacetate (TmDOTA(-))*. (2002) Int J Hyperthermia **18**, 165-179.
89. Hekmatyar, S. K., Hopewell, P., Pakin, S. K., Babsky, A. & Bansal, N. *Noninvasive MR thermometry using paramagnetic lanthanide complexes of 1,4,7,10-tetraazacyclododecane- $\alpha,\alpha',\alpha'',\alpha'''$ -tetramethyl-1,4,7,10-tetraacetic acid (DOTMA4-)*. (2005) Magnetic Resonance in Medicine **53**, 294-303.
90. Hekmatyar, S. K., Kerkhoff, R. M., Pakin, S. K., Hopewell, P. & Bansal, N. *Noninvasive thermometry using hyperfine-shifted MR signals from paramagnetic lanthanide complexes*. (2005) Int J Hyperthermia **21**, 561-574.
91. James, J. R., Gao, Y., Miller, M. A., Babsky, A. & Bansal, N. *Absolute temperature MR imaging with thulium 1,4,7,10-tetraazacyclododecane-1,4,7,10-tetramethyl-1,4,7,10-tetraacetic acid (TmDOTMA-)*. (2009) Magnetic Resonance in Medicine **62**, 550-556.
92. James, J. R., Gao, Y., Soon, V. C., Topper, S. M., Babsky, A. & Bansal, N. *Controlled radio-frequency hyperthermia using an MR scanner and simultaneous monitoring of temperature and therapy response by $(1)H$, $(23)Na$ and $(31)P$ magnetic resonance spectroscopy in subcutaneously implanted 9L-gliosarcoma*. (2010) Int J Hyperthermia **26**, 79-90.
93. Pakin, S. K., Hekmatyar, S. K., Hopewell, P., Babsky, A. & Bansal, N. *Non-invasive temperature imaging with thulium 1,4,7,10-tetraazacyclododecane-1,4,7,10-tetramethyl-1,4,7,10-tetraacetic acid (TmDOTMA-)*. (2006) NMR in Biomedicine **19**, 116-124.